Supplementary information:

A novel supermolecular preorganization route for improving g-C_3N_4/g-C_3N_4 metal-free homojunction photocatalysis

Chuang Liu, Xiaoli Dong*, Yuchen Hao, Xiuying Wang, Hongchao Ma and Xiufang Zhang

School of Light Industry and Chemical Engineering, Dalian Polytechnic University, #1 Qinggongyuan, Dalian 116034, P R China

E-mail: dongxiaoli65@163.com

This SI file includes:

Figs. S1 to S12

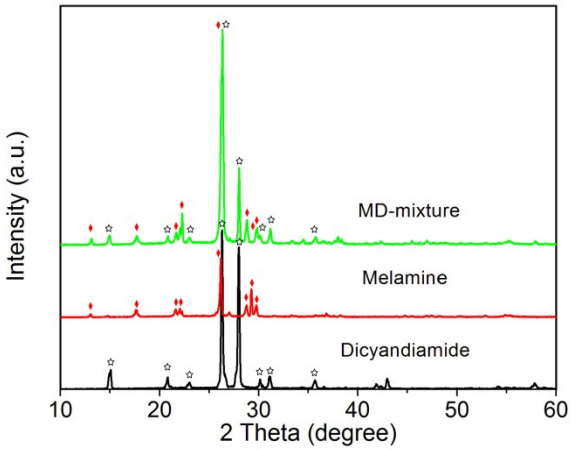

Figure S1 XRD patterns of dicyandiamide, melamine, and MD-mixture.

Figure S1 performed the X-ray diffraction patterns of dicyandiamide, melamine and MD-mixture. We find that the diffraction peaks of MD-mixture all can be found in the pristine dicyandiamide and melamine. There is also not found impurity peaks and peaks shift. It can be concluded that the conventional precursor complex is just simply stacking and mixing.

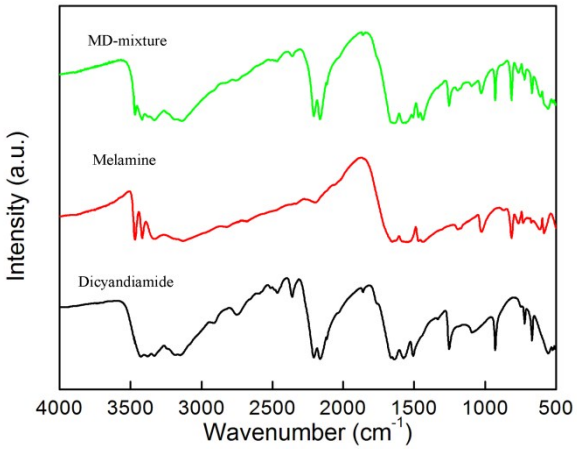

Figure S2 FT-IR spectra of dicyandiamide, melamine, and MD-mixture.

.

As shown in FT-IR spectra, the characteristic peaks of MD-mixture can be well indexed into melamine and dicyandiamide, further demonstrated the simple physical mixing of precursors, without chemical reaction occurring. For commercial melamine (red line), the peaks at 3331 cm^{-1}, 3180 cm^{-1} and 3129 cm^{-1} are attributed to the N-H stretching vibration. Meanwhile, the N-H deformation vibration could be observed at 1656 cm^{-1}.

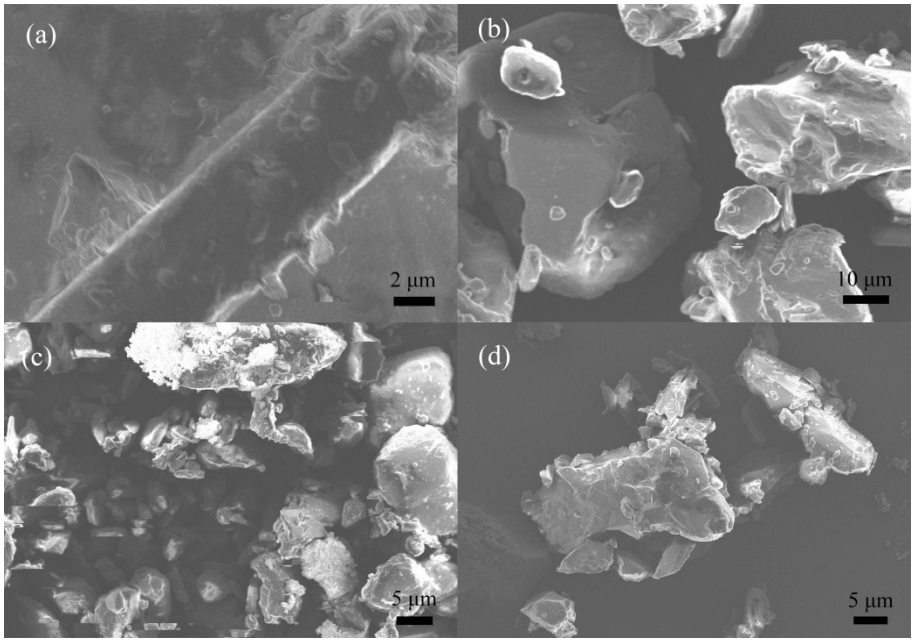

Figure S3 SEM images of (a) dicyandiamide, (b) melamine and (c, d) MD-mixture.

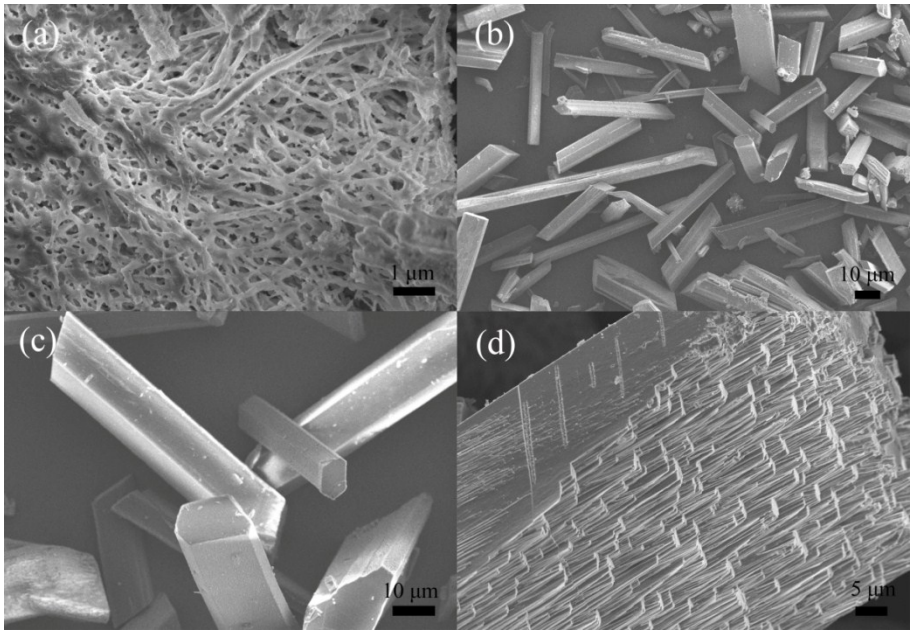

Figure S4 SEM images of H-D (a), H-M (b, c) and H-MD (d).

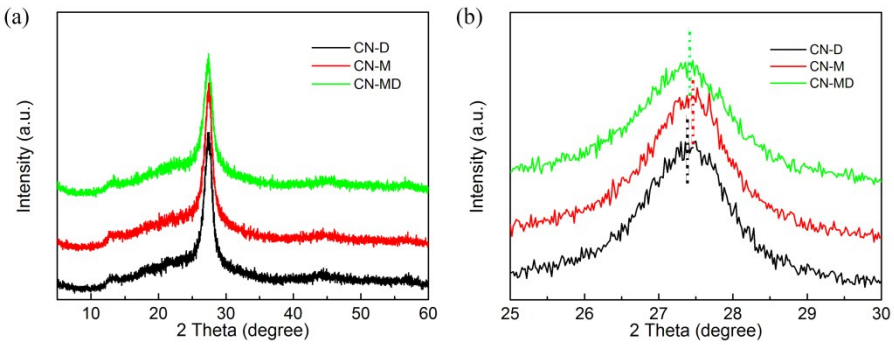

Figure S5 (a) XRD patterns of CN-D, CN-M, and CN-MD, and (b) enlarged profile of the dominant (002) peak.

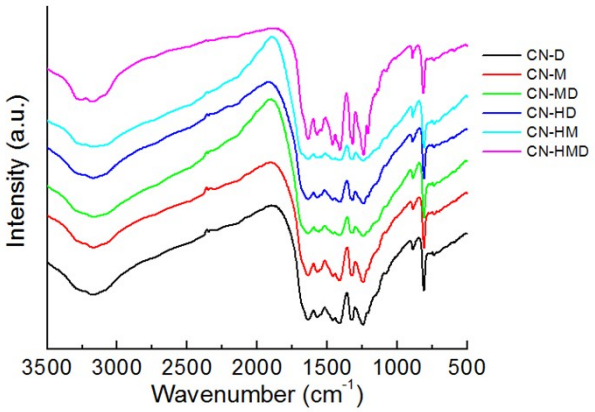

Figure S6 FT-IR spectra of all samples.

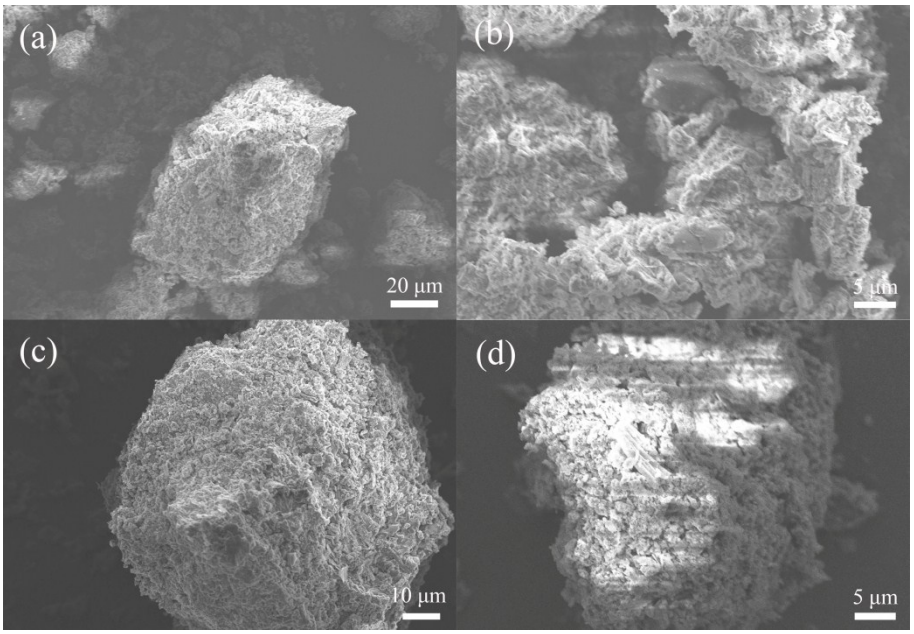

Figure S7 SEM images of (a) CN-D, (b) CN-M and (c, d) CN-MD.

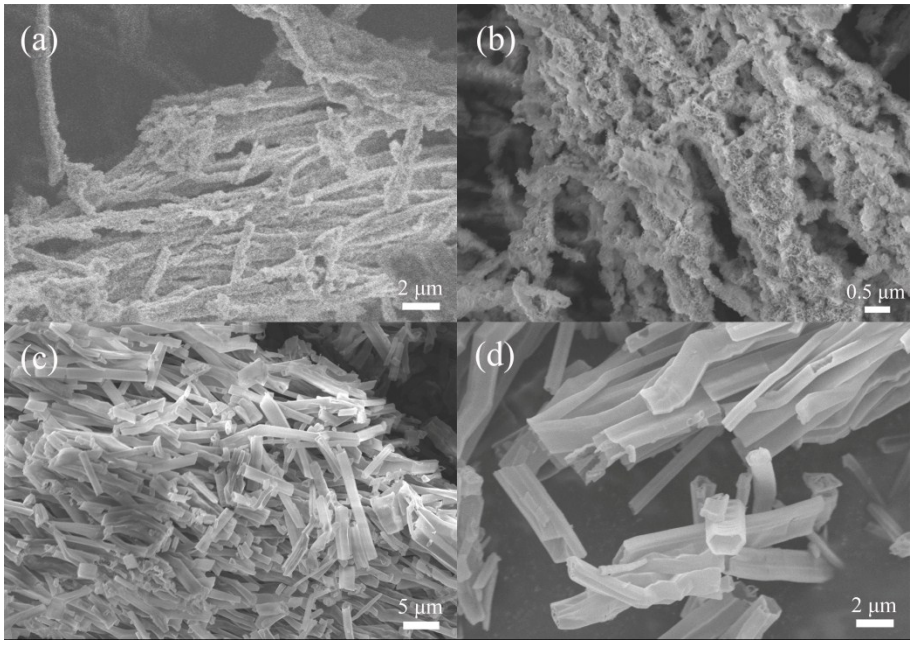

Figure S8 SEM images of (a, b) CN-HD and (c, b) CN-HM.

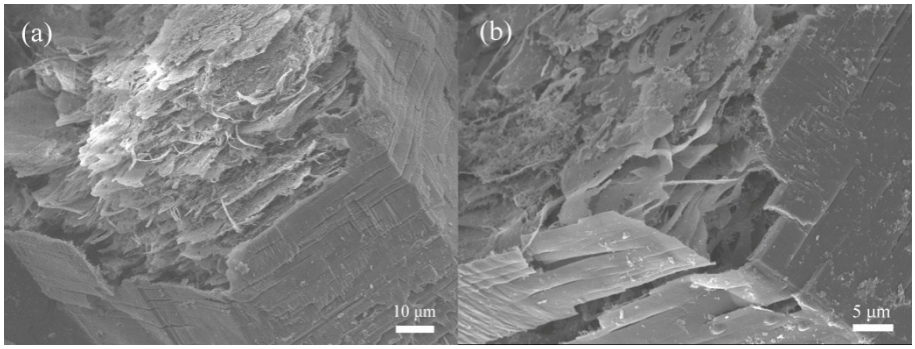

Figure S9 SEM images of (a, b) CN-HMD.

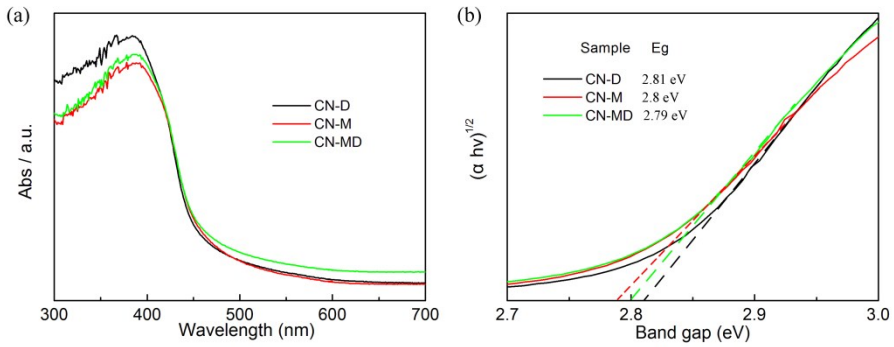

Figure S10 UV-Vis DRS (a) and plots of $(\alpha h\nu)^{1/2}$ vs photon energy (b) of CN-D, CN-M and CN-MD.

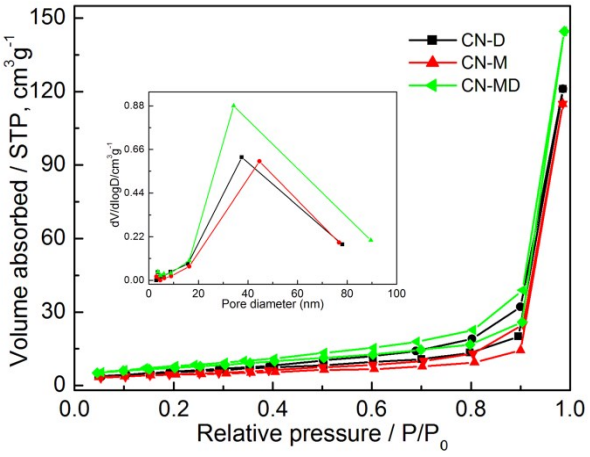

Figure S11 N_2 adsorption-desorption isotherms and the corresponding pore-size distribution curves of CN-D, CN-M and CN-MD

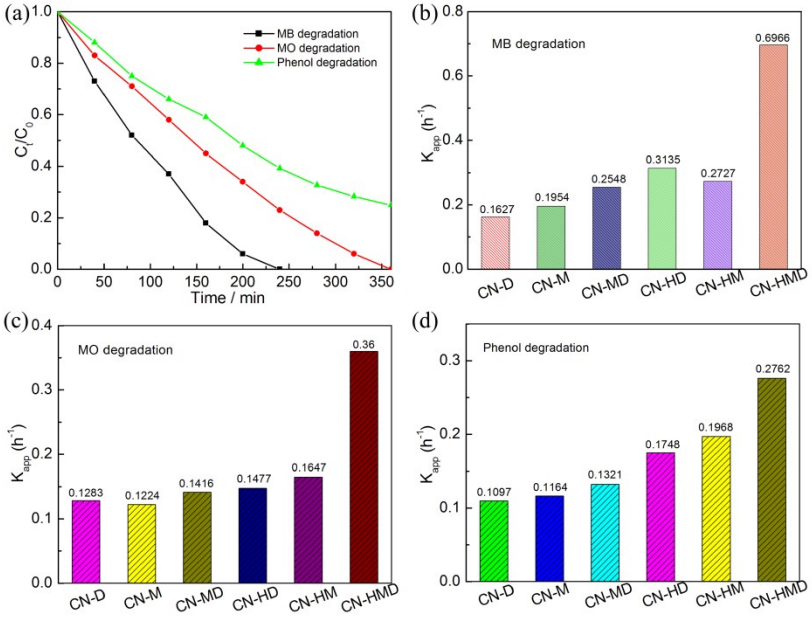

Figure S12 Photocatalytic degradation curve of contaminants (a) and corresponding K_{app} values over different samples under visible light (λ>420 nm) (b) MB, (c) MO and (d) phenol.